

We are IntechOpen, the world's leading publisher of Open Access books Built by scientists, for scientists

6,900

Open access books available

185,000

International authors and editors

200M

Downloads

Our authors are among the

154

Countries delivered to

TOP 1%

most cited scientists

12.2%

Contributors from top 500 universities



WEB OF SCIENCE™

Selection of our books indexed in the Book Citation Index
in Web of Science™ Core Collection (BKCI)

Interested in publishing with us?
Contact book.department@intechopen.com

Numbers displayed above are based on latest data collected.
For more information visit www.intechopen.com



Efficient Optimization of the Optoelectronic Performance in Chemically Deposited Thin Films

Andre Slonopas, Nibir K. Dhar, Herbert Ryan,
Jerome P. Ferrance, Pamela Norris and
Ashok K. Sood

Additional information is available at the end of the chapter

<http://dx.doi.org/10.5772/67315>

Abstract

Chemical deposition methodology is a well-understood and highly documented category of deposition techniques. In recent years, chemical bath deposition (CBD) and chemical vapor deposition (CVD) have garnered considerable attention as an effective alternative to other deposition methods. The applicability of CVD and CBD for industrial-sized operations is perhaps the most attractive aspect, in that thin-film deposition costs inversely scale with the processing batch size without loss of desirable optoelectronic properties in the materials. A downside of the method is that the optoelectronic characteristics of these films are highly susceptible to spurious deposition growth mechanisms. For example, increasing the temperature of the chemical deposition bath can shift the deposition mechanisms from ion-by-ion (two dimensional) precipitation to bulk solution cluster-by-cluster (three dimensional) formation which then deposit. This drastically changes the structural, optical, and electrical characteristics of CBD-deposited thin films. A similar phenomenon is observed in CVD deposited materials. Thus, it is of great interest to study the coupling between the deposition parameters and subsequent effects on film performance. Such studies have been conducted to elucidate the correlation between growth mechanisms and film performance. Here, we present a review of the current literature demonstrating that simple changes can be made in processing conditions to optimize the characteristics of these films for optoelectronic applications.

Keywords: chemical bath deposition, chemical vapor deposition, performance optimization, perovskites, optoelectronic performance

1. Introduction

The intent of this chapter is to cover the most recent advances achieved in optimization of chemically deposited thin films. The most prominent and widely used chemical deposition processes are chemical bath deposition (CBD) and chemical vapor deposition (CVD) methods. Recent breakthroughs in film optimizations relating to these methods will be the focus of this monograph.

Advanced thin films are the key enabler of the modern high-tech explosion. These materials find uses in military, defense, private, and commercial products with a truly limitless potential. It can be argued that every piece of electrical equipment, tool, hardware, and device commercially available relies, to some extent, on advanced processing of thin-film materials and our ability to scale those processes for cost-effective mass production.

Although CBD and CVD methods have been known since the 1940s and 1950s, respectively, the pursuit of cost reductions has driven recent research efforts in these fields [1, 2]. Specifically, the past decade has seen developments in the performance optimization of thin films by altering the deposition parameters. This has allowed for improved film characteristics without additional cost and spurred research into the growth and optimization of organic semiconductors [3–6]. Further, CVD and CBD have facilitated efficient device manufacturing by enabling systematic film layer depositions. Additional layers of a single material or of multiple materials may be deposited as necessary to grow monolithic structures for advanced applications. Such mesoscopic assemblies opened new doors for device manufacturing and optimization. These novel approaches are expected to further expand the capabilities of the current technology in a wide range of applications.

The recent advances in this particular field of science are far-reaching and extend beyond the scope of this chapter. This chapter reviews only the mainstream and high-impact achievements in chemically deposited thin films. Some of the current challenges and limitations of these methods are also addressed. This chapter is divided into two sections: the first section addresses the chemical bath deposition technique, structural and optoelectronic characterization, and performance of CBD deposited thin films; the second section deals with the chemical vapor deposition and performance and tunability of CVD deposited thin films. Tunability and deposition parameter optimization of film performance are addressed in both sections.

2. Chemical bath deposition (CBD)

The roots of chemical bath deposition extend back over a century [7]. It was initially shown that high-quality chalcogenides and oxides could be deposited using this simple cost-effective technique [8]. At the time, however, the semiconductor theory was decades away. Thus, only a few enthusiasts exhibited initial interest in the method. As the power of thin-film semiconductors was realized, the demand for such high-performance materials exploded. The market demand required a cost-effective method, which could sustain the production of high-quality

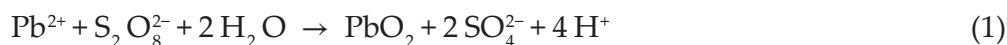
thin films. By this time, CBD was already a well-established process shown to produce highly crystalline structures and, thus, was a natural choice for such an application [9]. Research at that time showed that the method could also be applied for the deposition of metals, metallic alloys, chalcogenides, oxides, carbonates, and halides, all of which are an inherent part of next-generation organic semiconductors [10–12]. In more recent years, the process has been extended to deposit electron and hole transport layers (ETL and HTL, respectively), transparent conducting oxides (TCO), nanotubes, copper indium gallium selenide (CIGS) devices, and numerous other applications [13–17]. Further, the CBD method is inexpensive, easy to implement, convenient for large area depositions, and associated with highly favorable optoelectronic and structural properties [18, 19]. The power and the usefulness of the method cannot be overstated. Because of its broad applicability, CBD became a focus of numerous research groups.

2.1. CBD theoretical considerations

The underlying concept behind CBD is the rearrangement of the chemical constituents in the bath or already deposited on a substrate into functional crystalline structures during the chemical reactions. The original size of the chemical constituents can range from subatomic particles to microscale molecules. CBD finds a broad range of applications because it can be applied to a wide variety of chemicals. This concept is demonstrated further in the following examples.

(a) Electron exchange (redox)

Changes in oxidation numbers in elements during a chemical reaction indicate a redox reaction taking place. Such reactions take place in the CBD formations of metal, nonmetallic compounds, and oxide films, through direct oxidation or oxidative redox in which the electron exchange takes place among more than two elements. Insoluble lead dioxide [PbO₂], for example, forms from the oxidative redox of peroxydisulfate ion [S₂O₈²⁻] in water, as shown in Eq. (1) [20]:



(b) Ligand exchange

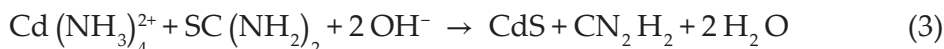
This type of reaction involves the exchange of ligands in a complex ion. Highly desired silicon dioxide [SiO₂] is precipitated using reaction 2 through the exchange of oxygen and fluorine ions. In general, this reaction holds an advantage in that it is generally more specific, allowing high selectivity in the produced compounds to be achieved [20]:



(c) Complex reaction

This type of reaction occurs by a coordinated exchange of complexes in a chemical bath, as illustrated in Eq. (3). Because of the potential for additional reactions, complex exchange reactions can have drawbacks that require advanced consideration. For example, due to its availability and low cost, thiourea [SC(NH₂)₂] is a common sulfur source used in CBD. Exchange

of sulfur from the thiourea requires complex decomposition and reaction. Although the stable molecule cyanamide $[\text{CN}_2\text{H}_2]$ is a common by-product of the thiourea decomposition, formation of reactive and toxic cyanide $[\text{CN}^-]$ has also been reported [21]. Such undesirable decompositions can have adverse effects on the overall deposition process:



The existence of numerous approaches to growing films in solutions is illustrated in the basic reactions discussed in Eqs. (1)–(3). It should also be inferred that careful consideration of each chemical reaction by-product is necessary to prevent contamination of the film or undesired waste products. The structural properties, precipitation rates, crystallinities, and—of greater interest—optical and electrical performance of materials can thus be controlled with careful planning. Perhaps, the most promising category of materials derived from a theoretical understanding of CBD has been organic semiconductors. Recently, CBD was used to crystallize $\text{CH}_3\text{NH}_3\text{PbI}_3$ perovskite powders for use in highly efficient organic-inorganic perovskite solar cells [22]. This would not have been possible without a deep theoretical understanding of the chemical reaction.

Reliably predicting film performance and controlling the deposition mechanisms is a formidable challenge. Charge carrier mobilities, for example, depend on the grain size, layer composition, porosity, interstitial trapping, doping, contaminants, diffusion lengths, substrate, bond lengths, and a plethora of other factors [23–25]. Recent deviations between continuum and atomistic level simulations stress this point further [26, 27].

However, it has been shown that it is possible to conduct an in situ study of the deposition parameters, deduce growth mechanisms, and reproduce the film performance from such simulations [28]. Accumulated experimental data are then utilized to converge atomistic models for accurate computational predictions [29]. The remainder of this section will discuss the accumulated experimental data on the corporeal control of the CBD process and its effects on film performance.

2.2. CBD experimental data

Two main deposition mechanisms dominate thin-film growth during CBD. The first, ion-by-ion (two dimensional) mechanism is the sequential reaction between ions to form clusters, shown in **Figure 1(a)**. Typically, this method produces highly stoichiometric crystals and can be finely controlled by the bath pH, temperature, and constituent concentrations. The second mechanism utilizing precipitation taking place in the bulk of the solution and known as cluster-by-cluster (three dimensional) growth is shown in **Figure 1(b)**. In general, there is less control over this latter mechanism, with the resulting structures deviating from stoichiometry calculations, often containing interstitial traps and producing unique optical and electrical material properties.

It is widely reported that the optoelectronic performance of chemically grown thin films is strongly dependent on the deposition mechanisms [30]. To evaluate this, the nonintrusive method of spectroscopic ellipsometry (SE) could be used to analyze the role of bath parameters on the deposition mechanisms. The films could then be subsequently analyzed using more intrusive methods to better understand the full scope of the relationship.

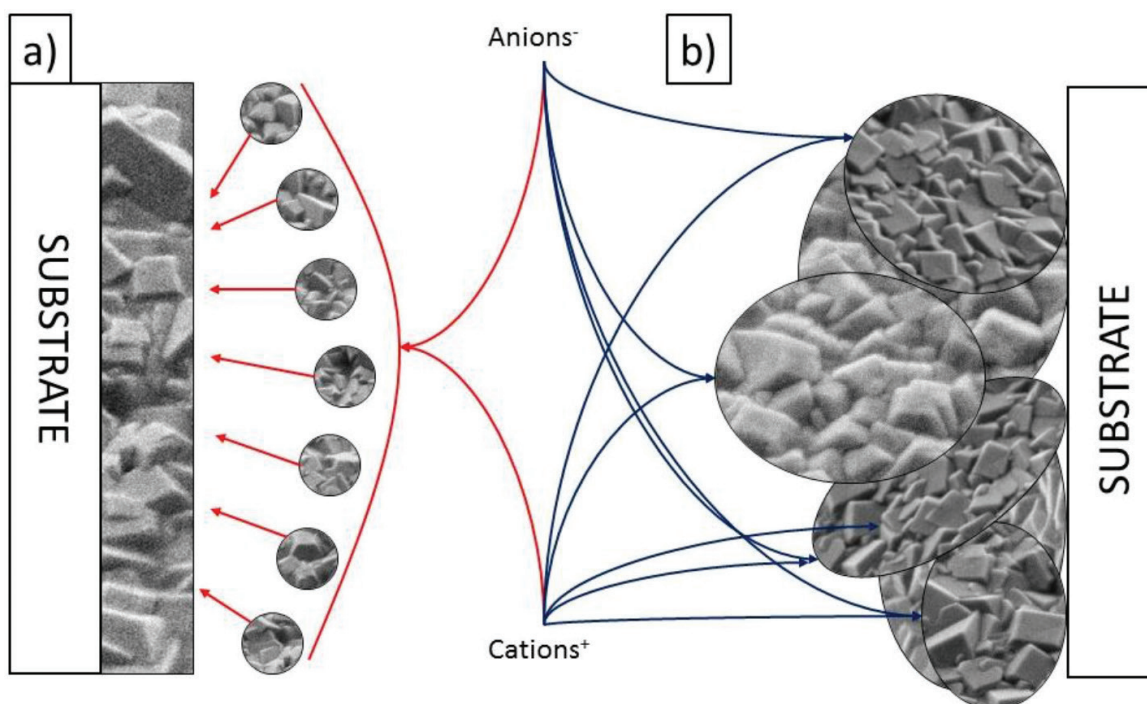


Figure 1. (a) Ion by ion and (b) cluster by cluster are the two dominating deposition mechanisms during chemical bath deposition. Ions permeate the solution precipitating on top of the substrate during growth in the ion-by-ion mechanism. As opposed to the cluster agglomerations forming in the bulk of the solution prior to attaching themselves to the substrate in the cluster-by-cluster mechanism.

SE analysis revealed three growth stages. The first stage was a short induction time, during which time little or no observable growth took place. Some of the material was observed to precipitate in the solution (although negligible amount showed adhesion to the substrate). The masses forming in the solution at this stage have not reached the critical diameter for crystallization. The second stage was a fairly linear growth period, dominated by the ion-by-ion mechanism.

This steady epitaxial growth produced highly compact stoichiometric films. The third stage was then dominated by the cluster-by-cluster mechanism in which clusters formed in the solution reached a critical size and could precipitate, producing a porous layer on top of the film. The porous layer typically established the surface roughness of the film. In some instances, this layer could be minimized by immediate washing following the chemical bath deposition [30]. Three distinct layers deposited by CBD are visible in the scanning electron microscope (SEM) images shown in **Figure 2**.

The nonintrusive SE measurements were used to study the effects of bath temperatures on the thickness of each layer. Data were collected on the films deposited at bath temperatures ranging from 55°C to 95°C. Physical models representative of the film structures were constructed consisting of three layers of quartz glass. The porosity and chemical composition of each layer were adjusted until a high correlation between the experimental and measured data was achieved [28].

It was found that at low bath temperature (i.e., 55°C) nearly 85% of the structure consisted of a highly stoichiometric and compact thin film. The porous surface layers in such films were

~1% of the entire structure thickness. This is indicative of substantial growth through the ion-by-ion deposition mechanism, which overwhelmingly dominates at low bath temperatures. Increase in the bath temperature was accompanied by a steady transition to the cluster-by-cluster mechanism. At a bath temperature of 95°C, the compact layer constituted ~60% of the entire structure thickness.



Figure 2. (a) Planar and (b) cross-sectional SEM reveal tight crystalline structure with three distinct layers.

The porous layer made up the majority of the rest of the film assembly [28]. These results indicate the coexistence of the two deposition mechanisms taking place in the bath during film formation. At lower temperatures, the ions are less likely to saturate the solution allowing the two-dimensional mechanism to dominate the film growth. As the temperature rises, the ion concentrations saturate and begin to form particulates in solution, causing the ion-by-ion mechanism to be supplemented by cluster-by-cluster growth.

It was realized that if a clear correlation between the optoelectronic performance of films and their growth mechanisms could be established, optimization of film performance through efficient means in the bath could be achieved. The high-impact nature of establishing this correlation prompted a significant amount of research on the topic.

One research topic of interest was the oxidation of the dangling bonds on the surface of stoichiometric crystalline films, which could be studied using X-ray photoelectron spectroscopy (XPS). XPS spectra of a CdS thin film as deposited on an n-InP substrate and a corresponding film after a 1-minute treatment with a buffer oxide etch (BOE) are shown in **Figure 3(a)** and **(b)**, respectively. The ratio of S:Cd prior to the 1 min BOE etch is found to be ~0.6 and increases to ~0.85 after the etch. These results reveal a thin (~30 nm) passivation CdO layer forming on top of the films [31]. Similar results have been widely reported in various materials deposited by CBD method [19]. Such stoichiometric structures are explained by the dangling bonds on the surface of the materials.

In general, the valence electrons deep in the bulk of the material are committed to the covalent bonds between the elements. Electrons near the film surface are less constrained, resulting in the dangling bonds. This allows for the ambient oxygen to oxidize the materials at or near

the surface, resulting in a thin layer of oxide being formed [19]. This thin oxidation layer prevents degradation of the films and introduces passivation properties in high-speed field-effect transistors. During subsequent depositions the layer acts as a buffer [31]. Oxidation removal from nanocrystalline thin films becomes an important step in efficiency enhancement of the monolithic structures, such as in CIGS. Similar passivation layer formations are not observed under three-dimensional (cluster by cluster) deposition mechanisms [28].

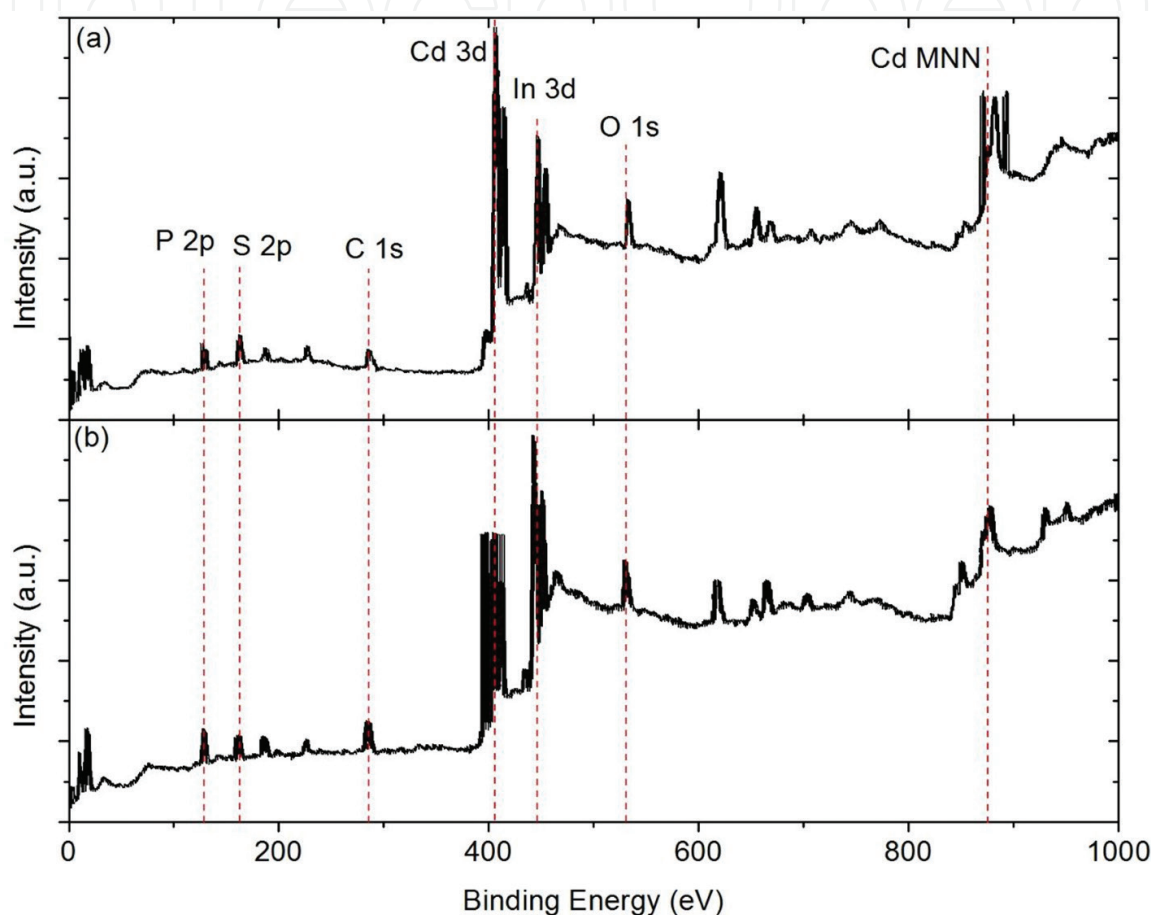


Figure 3. XPS spectra of an n-InP sample with (a) 2 min CdS deposition at 75°C and (b) CdO removal with 1 min of BOE immersion.

Optoelectronic performance of films is known to be heavily dependent on the crystalline structure of the materials [32, 33]. Crystallinity is of great interest for lattice matching in thin-film devices such as CIGS. Extensive X-ray diffraction (XRD) studies of film structures have been conducted and revealed that crystallinities are highly dependent on deposition temperatures. As an example, XRD data of CdS films deposited at various bath temperatures are shown in **Figure 4**. Lower deposition temperatures tend to deposit highly symmetric crystals—zinc blende (cubic) in the case of the CdS. As the bath temperatures are increased, a noticeable shift from symmetric to asymmetric structures is observed—wurtzite (hexagonal) structures in the case of CdS.

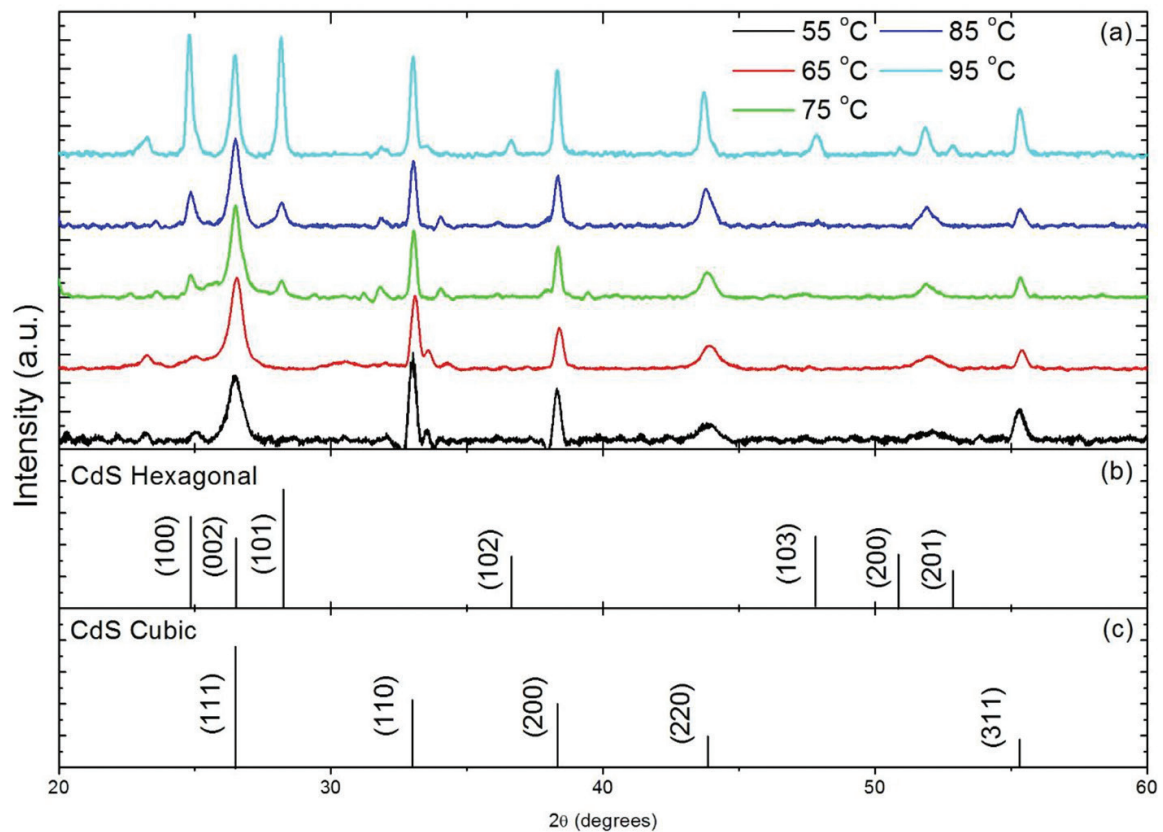


Figure 4. XRD patterns for CdS samples deposited at various bath temperatures. Spectra reveal a shift towards the hexagonal structures at higher deposition temperatures.

Under the three-dimensional deposition mechanism, much of the cluster agglomeration takes place in the bulk of the solution. These irregularly shaped clusters form the asymmetrical structures that attach themselves to the substrate. This is in contrast to the two-dimensional deposition mechanism which creates a uniform lateral expansion of the crystals. This contrast in film growth causes the structural differences produced by the two methods.

The cluster agglomeration, i.e., three-dimensional deposition mechanism, is expected to force interstitial trapping of the large cations in the bath. These trapped ions then act as dopants in the semiconductor, either releasing free electrons or introducing holes to the material. This drastically changes the optoelectronic performance of the films. Several groups pursued solid-state nuclear magnetic resonance (NMR) studies that substantiate this hypothesis. NMR analysis of three-dimensional deposited films reveals an increase in the peak intensity corresponding to cations intrinsic in the solution [28, 34].

These studies validate that the typically large cations of the inorganic thin films are trapped during the three-dimensional cluster agglomeration. Careful consideration of this phenomenon may be used to optimize film performance without the use of extrinsic dopants. Conversion efficiencies have been shown to improve nearly 5% by the careful use of interstitial trappings [34]. There is an additional challenge, however, that needs to be considered in order to achieve effective doping. Transition metals with large numbers of valence electrons are widely used as dopants in various inorganic thin films [35, 36].

However, work in this field demonstrated a limit in the doping efficiency for these metals [37, 38]. This is mainly due to formation of polyoxometalates between the transition metals and other ions in the chemical bath. The valence electrons that otherwise would be donated to the material are instead localized into formed complexes [39], which limit the doping efficiencies to ~1 donated electron per ion. This phenomenon is observed even in the materials with upward of seven valence electrons [37, 38]. Unpublished results from an ongoing study at the University of Virginia use interstitial iridium trapping to prove the possibility of overcoming theoretical doping efficiency limits.

Building on the aforementioned research, it is of great interest to tie the optoelectronic performance of the films to the growth mechanisms in the bath. Highly stoichiometric films grown by the ion-by-ion deposition mechanisms possess properties typical of intrinsic materials. Deviation from stoichiometry (i.e., introduction of the cluster-by-cluster mechanisms) noticeably changes the film characteristics. A case study of CdS is presented below.

Thin films of CdS fabricated under various deposition mechanisms were widely studied to show that the cluster-by-cluster growth mechanism produces a blend of crystalline structures. As previously mentioned, the XRD data revealed the formation of a blended cubic/hexagonal structures as temperature increased (**Figure 4**) [40, 41].

The refractive index (n) and extinction coefficient (k) over the range of deposition temperatures were obtained utilizing multiwavelength ellipsometer and are shown in **Figure 5(a)** and **(b)**, respectively. Two maxima in the refractive index located at ~280 and ~410 nm are visible in the films deposited at 55°C bath temperatures. There is a noticeable shift in the location of the maxima at higher bath temperatures. The two maxima in the latter cases are found at ~475 and ~275 nm wavelengths. These maxima are well studied and understood to be the fundamental absorption peaks in the transition along $\Gamma \rightarrow A$ Brillouin zone (BZ) boundaries in the CdS structure [42]. The shift in the locations of the maxima, however, testifies to the structural changes taking place in the crystals. At low bath temperatures, the location of the maxima is found to match expectations for the cubic structured CdS.

At higher deposition temperatures, however, the maxima are located slightly below the expected locations for the hexagonal structures [43, 44]. A noticeable variation in the change of the onset of the extinction coefficient is also observed. This is suggestive of a change in the optical band gap. Such a shift has been widely reported and is attributed to the cubic-hexagonal transitions taking place in the CdS film structure [45]. In a greater context, the multiwavelength analysis testifies that the ion-by-ion deposition mechanism favors the crystallization of highly symmetric structures, whereas the cluster-by-cluster deposition mechanism tends to produce asymmetry in crystallization and deviation from stoichiometry. However, the resulting structures are rarely of a single phase, and even at higher bath temperatures, the two-dimensional deposition mechanism contributes significantly to the overall structure of the film.

Changes in the crystallinity of the materials have a significant impact on the overall optical properties. Optical performance of the aforementioned CdS films was studied in an effort to understand the growth mechanism/optical performance relationship. Significant changes in

the reflectance and absorbance spectra are observed with the rise of the hexagonal phase in the film, as shown in **Figure 5(c)** and **(d)**, respectively. The three observed dips in the reflectance and absorbance data coincide with the valence band splits in Γ_9 , Γ_7 , and Γ_5 previously reported for CdS [46]. Reflectance is significantly higher in three-dimensionally grown films. The absorbance curve shows a steeper slope for the low deposition temperatures and a fairly flat absorption tail. These results suggest lower reflectance and higher absorbance of the symmetric structures deposited by two-dimensional mechanisms. Such results would be expected in the epitaxially grown films. The random distribution of the clusters produced by the three-dimensional mechanisms scatters light resulting in less favorable optical properties.

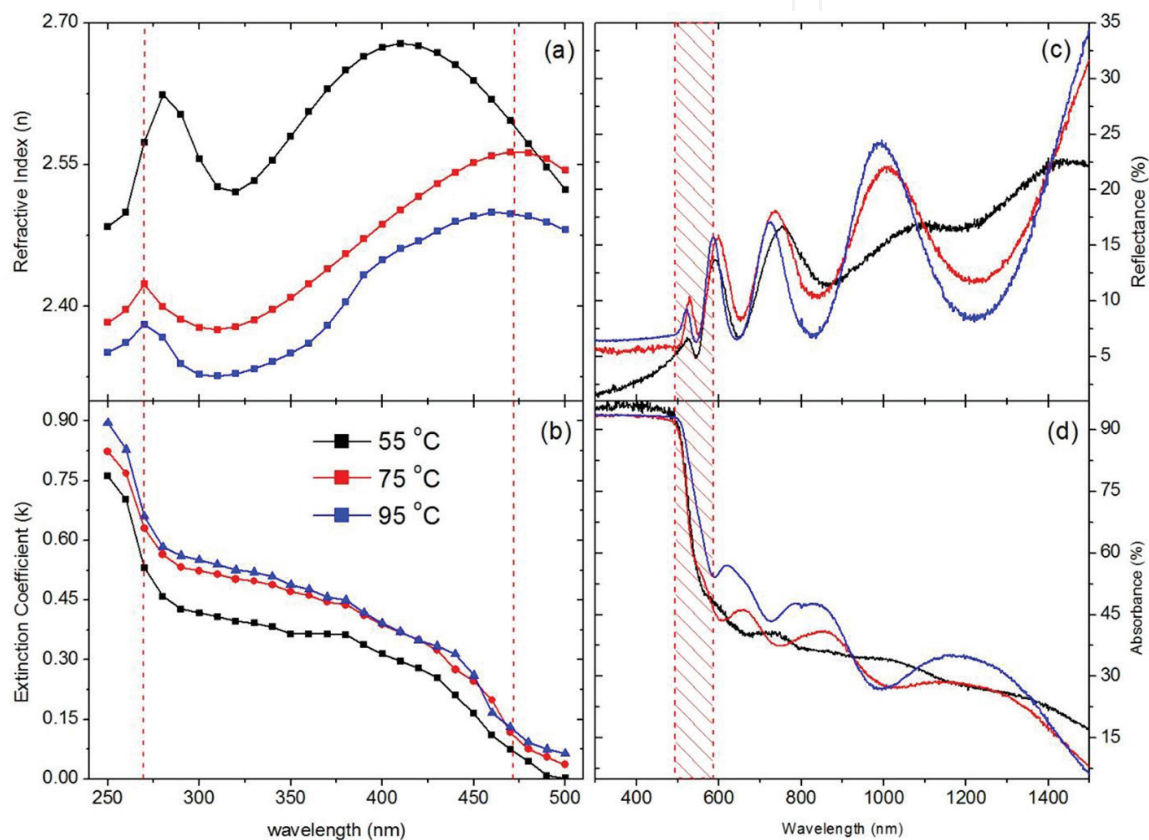


Figure 5. (a) Refractive index (n), (b) extinction coefficient (k), (c) reflectance, and (d) absorbance over a range of deposition temperatures.

Analysis of the electrical performance of CdS films deposited under different conditions was also conducted. Summary of the film's electrical properties is shown in **Table 1**. Cd:S ratios were computed from the XPS spectra and validated using energy-dispersive spectroscopy (EDS). Cd and S constituted the majority of the film composition. Traces of C, Ca, and Na contaminants were also observed but in negligible amounts. As can be seen from the data, the films deposited at low bath temperatures are highly stoichiometric.

This is evident from the 1:1 ratio between the Cd^{2+} and S^{2-} ions. Films deviate significantly from stoichiometry at higher bath temperatures, reaching ~ 1.67 Cd^{2+} ions per one S^{2-} . This is

understood from the previous discussion of the interstitial trapping. The large Cd^{2+} ions are caught in the lattice, offsetting the Cd:S ratio; correspondingly, the electrical performance was observed to be enhanced.

	Deposition temperatures (°C)		
	55	75	95
Ratio Cd:S	1:1	1:0.90	1:0.59
Optical band gap (eV)	2.43	2.45	2.49
n (cm^{-3}) $\times 10^{17}$	1.1	5.9	8.1
μ ($\text{cm}^2 \text{V}^{-1} \text{s}^{-1}$)	8.2	10.0	32.5
ρ (Ωcm)	33.5	30.7	9.3

Table 1. Deposition temperatures and film parameter summary [28].

For example, the carrier concentrations (n) increase over sevenfold. This is achieved without sacrificing the carrier mobility (μ) which also rises nearly four times. Resistivity (ρ) decreases over threefold as well. This phenomenon is contrary to the common empirical relationship between carrier concentrations and mobility [47, 48]. This is partially due to the larger grain sizes in the cluster-by-cluster grown lattices. More importantly, however, this is suggestive that unlike extrinsic doping, the interstitially trapped dopants contribute carriers without following the inverse proportional relationship between carrier concentrations and mobility. This is a significant result, allowing for semiconducting thin films to overcome current limitations.

2.3. CBD conclusions

From the presented research, it is evident that the growth mechanism during chemical bath deposition can follow several routes during the fabrication of thin film, which can affect their performance. Careful study of the deposition mechanisms allows for a controlled deposition of the film with the desired optoelectronic properties. Furthermore, control of the growth mechanism can allow for the theoretical doping limits to be overcome and for the exploitation of novel film regimes. All of this can be achieved simply by controlling the deposition temperature with negligible changes in the deposition costs.

3. Chemical vapor deposition (CVD)

CVD is another promising chemical deposition method for the production of high-quality thin films. Although this method was developed and studied since the 1960s, the recent interest in organic and two-dimensional semiconductors has reinvigorated the field. Perhaps, the most attractive characteristic of CVD is just how effective and versatile it can be [49]. Nanostructured

graphene, carbon nanotubes, $\text{CH}_3\text{NH}_3\text{PbI}_3$ perovskites with applications in optoelectronics, solid oxide fuel cells, batteries, sensors, and high-performance organic photovoltaics are all manufactured using CVD [50–52]. Moreover, this method has been shown to be adaptable for the deposition of a single-layer material and scalable for mass production [53, 54]. Another advantage of CVD is the conformity of the deposited films (i.e., the thicknesses and grain sizes near the substrate edges are comparable across the sample) [55]. Hence, such films can be deposited on elaborate shapes, inside underlying features, and in high aspect ratio holes. Thus, there are virtually no limits to the types of films that may be deposited using this method. CVD does not discriminate between transition metals, heavy metals, organics, and inorganics and has the ability to deposit all of these without distorting the structures of the films. Additionally, cost-effective distillation of the precursors allows for deposition of high-purity films. The power of this method cannot be overstated. Chemical vapor methods yield to chemical bath only in the areas of deposition surface size and the equipment cost.

3.1. CVD theoretical considerations

CVD is influenced by numerous factors. For example, the type, shape, size of the reactor, gas flow, flow rates, flow order, arrangements coating, and substrates all affect the overall deposition results and mechanisms. The deposition reactions themselves may require complicated reaction schemes, involving pyrolysis, reduction, oxidation, disproportionation, hydrolysis, or some combination of each [56]. Despite the various approaches to CVD, in general, the results are achieved in a linear sequence. First, reagents are applied to the substrate to create an initial kinetic barrier. This barrier needs to be permeated by the gaseous diffusion prior to the preliminary reactions. Initial absorption then takes place on the substrate surface followed by reactions among the chemical constituents which results in nucleation. As with the CBD study, careful consideration of the CVD experiments allows for an effective tunability of the film characteristics. Here, we present a short theoretical discussion.

In general, the flow of the gases is assumed to be laminar, with zero velocity near the surface of the substrate, and increasing linearly to a constant value at some distance from the substrate. In such an approximated case, the boundary layer theory (BLT) is used for the study of the reaction dynamics [57]. This approach couples the chemical and mass transport processes on the heated substrate surface with a gas flow.

The free energy of the chemical reaction is analogous to Gibbs free energy and may be easily shown to be

$$\Delta G = \sum_{i=1}^{\text{\#products}} \Delta G_{\text{products}} - \sum_{i=1}^{\text{\#reactants}} \Delta G_{\text{reactants}} \quad (4)$$

where ΔG is related to the equilibrium constant k_p :

$$\Delta G = 2.3RT \log(k_p) \quad (5)$$

Due to vapors utilized in the CVD process, the equilibrium constant is related to the partial pressures of the reactants and products. It is of greater interest, however, to relate the equilibrium constant in terms of concentrations. This is achieved using the ideal gas law [58]. The resulting free energy of the system consisting of g gaseous and s solid phases is thus

$$\Delta G = \sum_{i=1}^g \left[n_g \Delta G_g + RT \ln(P) + 2T \ln \left(\frac{n_g}{N_g} \right) \right] + \sum_{i=1}^s n_s \Delta G_s \quad (6)$$

where n_g and n_s are the number of moles of a particular reagent in the gaseous and solid state, respectively, and N_g is the total number of moles of all gaseous components. P and T are the total pressure and temperature, respectively. The ΔG_g and G_s are the free energy of formation at specific temperatures for the gaseous and solid species, respectively. Thus, the equation can be solved iteratively for the free energy minima, i.e., the point at which nucleation will commence. An analysis of the equation also reveals that the reagent concentrations can be offset by the pressure and temperature in the CVD chamber.

Hypothetically, it should be possible to conduct thin-film growth at low pressures and temperatures with high reagent concentrations; although such an approach would not be most efficient from the chemical perspective, it would, however, help alleviate the requirement for sophisticated equipment. Further, the low-temperature approach allows for the deposition of highly sought organic materials. Of course, there is also a limit to the operability temperatures, since at some pressure and temperature the molecular gases will liquefy.

The analogousness between the CBD and CVD methods should be obvious from the brief theoretical introduction. The free energy of the chemical reaction, Eq. (6), shows that reagent concentrations, pressure, and temperature are the control parameters of interest in CVD. Thus, similar to CBD method, the optoelectronic performance of the CVD grown films will depend heavily on the deposition parameters and mechanisms.

3.2. CVD experimental data

Low vapor temperatures result in less random scattering of reagents; thus, clusters, ~10 μm in diameter, form in the flowing gas prior to reaching the substrate. These clusters then coalesce on the surface of the substrate. The formation of CH_4/H_2 clusters is shown in **Figure 6(a)** and **(b)** [59]. The semisolid state of the clusters allows for coagulation with other clusters as they hit the substrate. In this case thermal diffusivity of the materials will determine the final structure of the materials [60]. In materials with low thermal diffusivity, e.g., organics, the structure resulting from the cluster-by-cluster deposition is similar to that of epitaxial growth. Consequently, materials with low thermal conductivity can be deposited at low temperatures. Thus, it follows that theoretically it may be possible to achieve firm crystalline structures and optimal optoelectronic performance of the films without the need for high deposition temperatures.

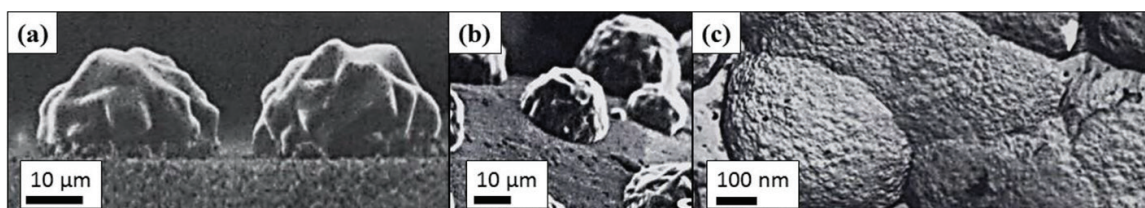


Figure 6. SEM images of carbon cluster formations on mirror-polished substrates.

Reagent concentrations also greatly affect the structural quality of the materials and their optoelectronic performance. For example, graphene deposited under high reagent concentrations showed high disorder, requiring synthesis of additional layers [61]. Raman analysis of graphene deposited under various methane concentrations partially reveals the causes behind the phenomenon, as shown in **Figure 7**. The data reveal an upshift of $\sim 5 \text{ cm}^{-1}$ and a downshift of $\sim 6 \text{ cm}^{-1}$ in the D and 2D peaks, respectively. Extensive research on such peak dispersions was shown to be caused by the formation of additional graphene layers [62].

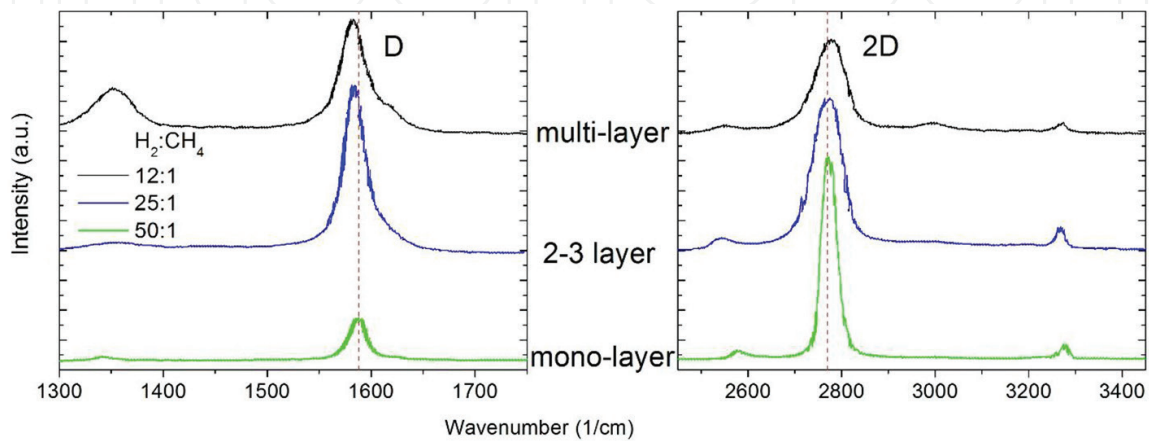


Figure 7. Raman spectra of CVD synthesized graphene with a Cu catalyst and SiO_2 substrates.

Furthermore, a significant increase in the D peak intensity is observed. This is typical of an increase in disorder [63]. The types of the disorders, whether layer or defect related, remain to be determined. Cumulatively, the results show that an increase in reagent concentrations produces mismatched layers and film defects. This causes anharmonic interactions between the phonons and electron-hole pairs [64], having a significant impact on the performance of such films. It is of great interest to conduct further research in minimizing layer mismatches and film defects. At present, this work is ongoing.

Preliminary results of the CVD flow rates and gas purity studies also show an effect on the optoelectronic performance of chemically deposited films. This research, however, is in the infancy stage and requires further analysis and effort.

There is a great potential for the efficient optimization of the optoelectronic performance of CVD deposited materials. Significant additional research into the deposition parameters and their effects on the growth mechanisms and optoelectronic performance will be required to fully understand the effects of each deposition parameter. It is expected that these issues will be resolved in the near future, allowing for effective optimization of these types of advanced materials.

3.3. CVD conclusions

In the optimization of CVD materials, thus far, the growth mechanisms have not been completely elucidated. There is, however, a strong correlation between the optoelectronic performance and

the deposition parameters. Much more research in the field of CVD modern-advanced materials is required but, once solved, will allow for an efficient optimization of such films.

4. Conclusion

This chapter discussed the growth mechanics, characteristics, and optimization of the optoelectronic performance in the chemically deposited materials. Two methods of interest are the chemical bath and chemical vapor depositions. Much more work has been completed in the field of CBD, but CVD is showing great promise in the deposition of novel advanced materials. The growth mechanisms are well understood for the chemical bath but remain to be elucidated for chemical vapor.

Once the growth mechanics are firmly established, it is possible to manipulate the chemical composition and other deposition parameters to efficiently optimize the optoelectronic film performance. Such results are abundant for the chemical bath, as is evident from the CdS case presented above, while for chemical vapor deposition, the research is ongoing. Each of these technologies is continuing to find uses in increasingly complicated manufacturing applications. It is expected that the ongoing research will enable new technologies for a wide variety of applications.

Acknowledgements

The authors are grateful to the contributions of many researchers at the University of Virginia and the NVEDS, who graciously provided their results and experimental data for the publication. These contributions are paramount in advancing the development of novel thin films and manufacturing methods.

Author details

Andre Slonopas^{1*}, Nibir K. Dhar¹, Herbert Ryan², Jerome P. Ferrance³, Pamela Norris⁴ and Ashok K. Sood⁵

*Address all correspondence to: as2vd@virginia.edu

1 U.S. Army RDECOM CERDEC Night Vision and Electronic Sensors Directorate, Fort Belvoir, VA, USA

2 Bitome Inc., Boston, MA, USA

3 Department of Chemistry, University of Virginia, Charlottesville, VA, USA

4 Department of Mechanical and Aerospace Engineering, University of Virginia, Charlottesville, VA, USA

5 Magnolia Optical Technologies, Inc., Woburn, MA, USA

References

- [1] Dobkin D., Zuraw M. K. Principles of Chemical Vapor Deposition: What's Going on Inside the Reactor. 1st ed. NY: Springer Science; 2013. 242 p. DOI: 10.1007/978-94-017-0369-7.
- [2] Nielsen A. E. Kinetics of Precipitation (International Series of Monographs on Analytical Chemistry). 1st ed. NY: Pergamon Press; 1964.
- [3] Schwartz R. W. Chemical solution deposition of perovskite thin films. *Chemistry of Materials*. 1997;9:2325–2340. DOI: 10.1021/cm970286f.
- [4] Tavakoli M. M., Gu L., Gao Y., Reckmeier C., He J., Rogach A. L., Yao Y., Fan Z. Fabrication of efficient planar perovskite solar cells using a one-step chemical vapor deposition method. *Scientific Reports*. 2015;4:14083. DOI: 10.1038/srep14083.
- [5] Taima T., Shahiduzzaman M., Yamamoto K., Furumoto Y., Kuwabara T., Takahashi K. Planar heterojunction type perovskite solar cells based on TiO_x compact layer fabricated by chemical bath deposition. *Proceedings SPIE 9749. Oxide-based Materials and Devices VII*. 2016.
- [6] Chow L., Wang H., Kleckley S., Daly T. K., Buseck P. R. Fullerene formation during production of chemical vapor deposited diamond. *Applied Physics Letters*. 1995;66:430. DOI: 10.1063/1.114046.
- [7] Puscher C., Water glass as a solvent for coralline. *Chemical News*. 1870;21:239.
- [8] Lincot D., Hodes G. Overview of history and present trends in chemical bath deposition of thin solid films and structures. *ChemInform*. 2008;39. DOI: 10.1002/chin.200809234.
- [9] Goldstein A. W., Rostoker W., Schossberger F., Gutzeit G. Structure of chemically deposited nickel. *Journal of the Electrochemical Society*. 1957;104:104–110. DOI: 10.1149/1.2428503.
- [10] Chopra K. L., Kainthla R. C., Pandya D. K., Thakoor A. P. Chemical solution deposition of inorganic films. *Physics of Thin Films*. 1982;12:167–235. DOI: 10.1016/S0079-1970(13)70010-0.
- [11] Lincot D., Froment M., Hubert C. Chemical deposition of chalcogenide thin films from solution. In: Alkire R. C., Kolb D. M., editors. *Advances in Electrochemical Science and Engineering*. Wiley Online Library; 2008. pp. 165–235. DOI: 10.1002/9783527616800.ch3.
- [12] Verdieck R. G., Yntema L. F. The electrochemistry of baths of fused aluminum halides. IV. *The Journal of Physical Chemistry*. 1944;48:268–279. DOI: 10.1021/j150437a005.
- [13] Yu X., Marks T. J., Facchetti A. Metal oxides for optoelectronic applications. *Nature Materials*. 2016;15:383–396. DOI: 10.1038/nmat4599.
- [14] Steirer X. K., Chesin J. P., Widjonarko N. E., Olson D. C. Solution deposited NiO thin-films as hole transport layers in organic photovoltaics. *Organic Electronics*. 2010;11:1414–1418. DOI: 10.1016/j.orgel.2010.05.008.
- [15] Elen K., Capon B., De Dobbelaere C., Dewulf D., Peys N., Detavernier C., Hardy A., Van Bael M. K. Transparent conducting oxide films of group V doped titania prepared by

- aqueous chemical solution deposition. *Thin Solid Films*. 2014;555:33–38. DOI: 10.1016/j.tsf.2013.05.104.
- [16] Zhang H., Ma X., Xu J., Yang D. Synthesis of CdS nanotubes by chemical bath deposition. *Journal of Crystal Growth*. 2004;263:372–376. DOI: 10.1016/j.jcrysgro.2003.11.090.
- [17] Nakada T., Kunioka A. Direct evidence of Cd diffusion into Cu(In,Ga)Se₂/Cu(In,Ga)Se₂ thin films during chemical-bath deposition process of CdS films. *Applied Physics Letters*. 1999;74:2444. DOI: 10.1021/cm970351l.
- [18] Moutinho H. R., Albin D., Yan Y., Dhere R. G., Li X., Perkins C., Jiang C. S., To B., Al-Jassim M. M. Deposition and properties of CBD and CSS CdS thin films for solar cell application. *Thin Solid Films*. 2003;436:175–180. DOI: 10.1016/S0040-6090(03)00646-1.
- [19] Slonopas A., Alijabbari N., Saltonstall C., Globus T., Norris P. Chemically deposited nanocrystalline lead sulfide thin films with tunable properties for use in photovoltaics. *Electrochimica Acta*. 2015;151:140–149. DOI: 10.1016/j.electacta.2014.11.021.
- [20] Mindt W. Electroless deposition of certain metal oxides. *Journal of the Electrochemical Society*. 1970;117:615–618. DOI: 10.1149/1.2407588.
- [21] Mitzi D. B., Yuan M., Liu W., Kellock A. J., Chey J. S., Deline V. A high-efficiency solution-deposited thin-film photovoltaic device. *Advanced Materials*. 2008;20:3657–3662. DOI: 10.1002/adma.200800555.
- [22] Slonopas A., Foley B. J., Choi J. J., Gupta M. C. Charge transport in bulk CH₃NH₃PbI₃ perovskite. *Journal of Applied Physics*. 2016;119:074101. DOI: 10.1063/1.4941532.
- [23] Law M. E., Lian M., Burk D. E. Self-consistent model of minority-carrier lifetime, diffusion length, and mobility. *IEEE Electron Device Letters*. 2002;12:401–403.
- [24] Liu Y., Gibbs M., Puthussery J., Gaik S., Ihly R., Hillhouse H. W., Law M. Dependence of carrier mobility on nanocrystal size and ligand length in PbSe nanocrystal solids. *Nano Letters*. 2010;10:1960–1969. DOI: 10.1021/nl101284k.
- [25] Takagi S., Toriumi A., Iwase M. On the universality of inversion layer mobility in Si MOSFET's: Part I—effects of substrate impurity concentration. *IEEE Transactions on Electronic Devices*. 1994;41:2357–2362. DOI: 10.1109/16.337449.
- [26] Weinan E., Zhongyi H.. Matching conditions in atomistic-continuum modeling of materials. *Physical Review Letters*. 2001;87:135501. DOI: 10.1103/PhysRevLett.87.135501.
- [27] Stukowski A. Computational analysis methods in atomistic modeling of crystals. *The Journal of The Minerals: Metals & Materials Society (TMS)*. 2014;66:399–407. DOI: 10.1007/s11837-013-0827-5.
- [28] Slonopas A., Ryan H., Foley B., Sun Z., Sun K., Globus T., Norris P. Growth mechanisms and their effects on the optoelectronic properties of CdS thin films prepared by chemical bath deposition. *Materials Science in Semiconductor Processing*. 2016;52:24–31. DOI: 10.1016/j.mssp.2016.05.011.

- [29] Frost J. M., Butler K. T., Brivio F., Hendon C. H., Van Schilfgaarde M., Walsh A. Atomistic origins of high-performance in hybrid halide perovskite solar cells. *Nano Letters*. 2014;14:2584–2590. DOI: 10.1021/nl500390f.
- [30] Hodes G. *Chemical Solution Deposition of Semiconductor Films*. NY: Marcel Dekker Inc; 2002.
- [31] Dauplaise H. M., Vaccaro K., Davis A., Ramseyer G. O., Lorenzo J. O. Analysis of thin CdS layers on InP for improved metal–insulator–semiconductor devices. *Journal of Applied Physics*. 1996;80:2873. DOI: 10.1063/1.363139.
- [32] Shinde S. S., Shinde P. S., Bhosale C. H., Rajpure K. Y. Optoelectronic properties of sprayed transparent and conducting indium doped zinc oxide thin films. *Journal of Physics D: Applied Physics*. 2008;41:105109.
- [33] Sebastian P. J., Calixto M. E., Bhattacharya R. N., Noufi R. CIS and CIGS based photovoltaic structures developed from electrodeposited precursors. *Solar Energy Materials and Solar Cells*. 1999;59:125–135. DOI: 10.1016/S0927-0248(99)00037-9.
- [34] Neuschitzer M., Sanchez Y., Olar T., Thersleff T., Lopez-Marino S., Oliva F., Espindola-Rodriguez M., Xie H., Placidi M., Izquierdo-Roca V., Lauer mann I., Leifer K., Perez-Rodriguez A., Saucedo E. Complex surface chemistry of kesterites: Cu/Zn reordering after low temperature postdeposition annealing and its role in high performance devices. *Chemistry of Materials*. 2015;27:5279–5287. DOI: 10.1021/acs.chemmater.5b01473.
- [35] Sebastian P. J. p-type CdS thin films formed by *in situ* Cu doping in the chemical bath. *Applied Physics Letters*. 1993;62:2956. DOI: 10.1063/1.109181.
- [36] Goudarzi A., Aval G. M., Park S. S., Choi M. C., Sahraei R., Ullah H. M., Avane A., Ha C. S. Low-temperature growth of nanocrystalline Mn-doped ZnS thin films prepared by chemical bath deposition and optical properties. *Chemistry of Materials*. 2009;21:2375–2385. DOI: 10.1021/cm803329w.
- [37] Lozano O., Chen Q. Y., Wadekar P. V., Seo H. W., Chinta P. V., Chu L. H., Tu L. W., Lo I., Yeh S. W., Ho N. J., Chuang F. C., Jang D., Wijesundera D., Chu W. K. Factors limiting the doping efficiency of transparent conductors: a case study of Nb-doped In₂O₃ epitaxial thin-films. *Solar Energy Materials and Solar Cells*. 2013;113:171–178. DOI: 10.1016/j.solmat.2013.02.006.
- [38] Slonopas A., Melia M., Xie K., Globus T., Fitz-Gerald J. M., Norris P. Factors limiting doping efficiency of Iridium in pulsed laser deposited TiO₂ transparent conducting oxide. *Journal of Material Science*. 2016;51:8995–9004. DOI: 10.1007/s10853-016-0152-9.
- [39] Siedle A. R., Newmark R. A., Brown-Wesley K. A., Skarjune R. P., Haddad L. C., Hodgson K. O., Roe A. L. Solid-state organometallic chemistry of molecular metal oxide clusters: carbon-hydrogen activation by an iridium polyoxometalate. *Organometallics*. 1988;7:2078–2079. DOI: 10.1021/om00099a037.
- [40] Joint Committee on Powder Diffraction Standards (JCPDS). Card 10–0454, CdS (cubic), 1999.

- [41] Joint Committee on Powder Diffraction Standards (JCPDS). Card 6–0314, CdS (hexagonal), 1999.
- [42] Zelaya-Angel O., Hernandez L., De Melo O., Alvarado-Gil J. J., Lozada-Morales R., Falcony C., Vargas H., Ramirez-Bon R. Band-gap shift in CdS: phase transition from cubic to hexagonal on thermal annealing. *Vacuum*. 1995;46:1083–1085. DOI: 10.1016/0042-207X(95)00111-5.
- [43] Jensen B., Torabi A. Refractive index of hexagonal II–VI compounds CdSe, CdS, and CdSexS1-x. *Journal of the Optical Society of America B*. 1986;3:857–863. DOI:10.1364/JOSAB.3.000857.
- [44] Al Kuhaimi A. S. Influence of preparation technique on the structural, optical and electrical properties of polycrystalline CdS films. *Vacuum*. 1998;51:349–355. DOI:10.1016/S0042-207X(98)00112-2.
- [45] Pal U., Silva-Gonzales R., Martinez-Montes G., Gracia-Gimenez M., Vidal M. A., Torres S. Optical characterization of vacuum evaporated cadmium sulfide films. *Thin Solid Films*. 1997;305:345–350. DOI:10.1016/S0040-6090(97)00124-7.
- [46] Seto S. Photoluminescence, reflectance and photorefectance spectra in CdS epilayers on Si(111) substrates. *Japanese Journal of Applied Physics*. 2005;44.
- [47] Hilsum C. Simple empirical relationship between mobility and carrier concentration. *Electronics Letters*. 1974;10:259–260.
- [48] Masetti G., Severi M., Solmi S. Modeling of carrier mobility against carrier concentration in arsenic-, phosphorus-, and boron-doped silicon. *IEEE Transactions on Electron Devices*. 1983;30. DOI:10.1109/T-ED.1983.21207.
- [49] Liu Y., Liu M. A highly sensitive and fast-responding SnO₂ sensor fabricated by combustion chemical vapor deposition. *Chemistry of Materials*. 2005;17:3997–4000. DOI:10.1021/cm050451o.
- [50] Liu Y., Zha S., Liu M. Novel nanostructured electrodes for solid oxide fuel cells fabricated by combustion chemical vapor deposition (CVD). *Advanced Materials*. 2004;16:256–260. DOI:10.1002/adma.200305767.
- [51] Liu Y., Zha S., Liu M. Nanocomposite electrodes fabricated by a particle-solution spraying process for low-temperature SOFCs. *Chemistry of Materials*. 2004;16:3502–3506. DOI:10.1021/cm049583s.
- [52] Leyden M. R., Ono L. K., Raga S. R., Kato Y., Wang S., Qi Y. High performance perovskite solar cells by hybrid chemical vapor deposition. *Journal of Materials Chemistry A*. 2014;2:18742–18745. DOI: 10.1039/C4TA04385E.
- [53] Gomez L., Zhang Y., Kumar A., Zhou C. Synthesis, transfer, and devices of single- and few-layer graphene by chemical vapor deposition. *IEEE Transactions on Nanotechnology*. 2009;8:135–138. DOI:10.1109/TNANO.2009.2013620.
- [54] Kumar M., Ando Y. Chemical vapor deposition of carbon nanotubes. *Journal of Nanoscience and Nanotechnology*. 2010;10:3739–3758. DOI:10.1166/jnn.2010.2939.

- [55] Thomann A. L., Vahlas C., Aloui L., Samelor D., Caillard A., Shaharil N., Blanc R., Millon E. Conformity of aluminum thin films deposited onto micro-patterned silicon wafers by pulsed laser deposition, magnetron sputtering, and CVD. *Chemical Vapor Deposition*. 2011;17:366–374. DOI:10.1002/cvde.201106936.
- [56] Yee K. K. Protective coatings for metals by chemical vapour deposition. *International Metals Review*. 2013;23:19–42. DOI:10.1179/imtr.1978.23.1.19.
- [57] Spear K. E. Principles and applications of chemical vapor deposition (CVD). *Pure and Applied Chemistry*. 1982;54:1297–1311.
- [58] Petrucci R. H., Harwood W. S., Herring G. E., Madura J. *General Chemistry: Principles and Modern Application*. 9th ed.. Newark, NJ: Prentice Hall; 2016.
- [59] Melnikova V. The cluster growth mechanism of nanostructured diamond. In: Veziroglu T. N., Zaginaichenko Y. S., Schur V. D., Baranowski B., Shpak P. A., Skorokhod V. V. *Hydrogen Materials Science and Chemistry of Carbon Nanomaterials*. NY: Springer; 2007. pp. 557–562. DOI:10.1007/1-4020-2669-2_64.
- [60] Murakami T. N., Kijitori Y., Kawashima N., Miyasaka T. Low temperature preparation of mesoporous TiO₂ films for efficient dye-sensitized photoelectrode by chemical vapor deposition combined with UV light irradiation. *Journal of Photochemistry and Photobiology A: Chemistry*. 2004;164:187–191. DOI:10.1016/j.jphotochem.2003.11.021.
- [61] Bhaviripudi S., Jia X., Dresselhaus M. L., Kong J. Role of kinetic factors in chemical vapor deposition synthesis of uniform large area graphene using copper catalyst. *Nano Letters*. 2010;10:4128–4133. DOI:10.1021/nl102355e.
- [62] Pocsik I., Hundhausen M., Koos M., Ley L. Origin of the D peak in the Raman spectrum of microcrystalline graphite. *Journal of Non-Crystalline Solids*. 1998;227–230:1083–1086. DOI:10.1016/S0022-3093(98)00349-4.
- [63] Tuinstra F., Koenig J. L. Raman spectrum of graphite. *The Journal of Chemical Physics*. 1970;53:1126. DOI:10.1063/1.1674108.
- [64] Ferrari A. C., Robertson J. Interpretation of Raman spectra of disordered and amorphous carbon. *Physical Review B*. 1999;61:14095. DOI:10.1103/PhysRevB.61.14095.